SUPPLEMENTAL MATERIALS

Expanded Materials and Methods:

Animals

Mouse protocols were approved by the Institutional Animal Care and Use Committee of University of Texas Southwestern Medical Center (UTSW). Mice were on pure C57BL/6 background and maintained in 12:12 hours light:dark cycle in temperature-controlled mouse facilities. All animals had free access to water and chow food (Teklad, #2916). To achieve cardiac specific knockout of ATF4, $ATF4^{F/F}$ mice[22] were crossed with cardiomyocyte specific Cre (αMHC-Cre) mice.[18, 19, 34] Genotyping primers are listed in Supplemental Table S1.

Transverse aortic constriction (TAC)

Transverse aortic constriction (TAC)[14] was performed on male mice of approximately 8 weeks old (23-25 grams). Briefly, anesthesia was achieved by injection of ketamine (100 mg/kg, I.P.) and xylazine (5 mg/kg, I.P.). Instruments, supplies, and suture materials were sterilized before use. Oral intubation was conducted. An incision in the anterior neck was created to reveal the trachea and facilitate cannulation of the upper airway. Body temperature, respiratory rate, and heart rate were recorded. The aortic arch was accessed via left lateral thoracotomy. The suture of 5-0 silk was used to ligate the aorta between the innominate and left carotid arteries and an overlying 26G needle. The needle was then removed, leaving a discrete region of stenosis. Finally, the chest was closed, and mice were observed during recovery from anesthesia. Sham operation was similarly conducted without suture ligation. Surgeons were blind to genotypes and treatment groups.

De-transverse aortic constriction (deTAC)

After 3 days of TAC, deTAC was performed. Briefly, anesthesia was achieved by injection of ketamine (100 mg/kg, I.P.) and xylazine (5 mg/kg, I.P.). The aortic arch on the left lateral thoracotomy was reopen. The 5-0 silk suture was then cut off and removed from the aorta. Finally, the chest was closed. Mice were observed during recovery. A week later, the heart was harvested for further analyses.

Aortocaval fistula (ACF) model

ACF model was generated in wild-type mice as before.[48] Briefly, a ventral abdominal laparotomy was performed to expose the aorta and caudal vena cava approximately 1.5 cm below the renal arteries. The overlying tissue was removed by blunt dissection and vessels were exposed. The proximal and distal vessels of the puncture site were occluded, and an 18-gauge needle was inserted into the exposed abdominal aorta and advanced through the medial wall into the vena cava to create fistula. The needle was then removed, and the puncture site was immediately sealed with cyanoacrylate. The observation of the pulsatile flow of oxygenated blood into the vena cava was used to confirm successful operation. The abdominal musculature and skin incisions were closed with absorbable suture and tissue glue. Mice were sacrificed a week later, and the heart was collected for further analyses.

Echocardiography

Unconstrained, conscious mice were used to measure cardiac function with echocardiography (Visual Sonics, #Vevo 2100) as previously described.[19] M-mode images of the short-axis view at the level of papillary muscles were captured and used to analyze and calculate various cardiac functional parameters. Heart rate was recorded. Left ventricular internal diameters (in mm) at end diastole (LVID, diastolic) and end systole (LVID, systolic) were determined with M-mode recordings. Fractional shortening (%) and ejection fraction (%) were calculated.

Neonatal rat ventricular myocyte isolation

Neonatal rat ventricular myocytes (NRVMs) were isolated from ventricles of 1 to 2 days old Sprague-Dawley rats (Charles River Laboratories) using a cardiomyocyte isolation kit (Cellutron, #NC-6031).[19] Briefly, after 2 hours of pre-plating to remove fibroblasts, cardiomyocytes were plated at a density of 1,250 cells/mm^2 in plating medium (DMEM/M199=3:1) containing 5% FBS, 10% horse serum, 1% penicillin/streptomycin, and bromodeoxyuridine (BrdU, 100 μM). BrdU was included to suppress fibroblast proliferation in culture. After another 24 hours of plating, NRVMs were washed with PBS and cultured in serum-reduced medium (DMEM/M199=3:1, 1% FBS, 1% penicillin/streptomycin, 100 μM BrdU). Twenty-four hours later, NRVMs were incubated in serum-free medium (DMEM/M199=3:1). Cells were then used for various treatments, including siRNA transfection and adenovirus infection.

Flow cytometry analysis of reactive oxygen species

For mitochondrial superoxide detection, MitoSOX Red mitochondrial superoxide indicator (ThermoFisher Scientific, #M36008) was used. MitoSOX Red signal was detected using a FACScan flow cytometer and results were analyzed with Flowjo 10.7.2. Cytosolic general oxidative stress was measured by CM-H_2DCFDA (ThermoFisher Scientific, #C6827) staining and quantified with Flowjo 10.7.2.

NADPH and NADP$^+$ measurements

Concentrations of NADPH and NADP$^+$ were measured using an NADPH/NADP$^+$ colorimetric assay kit (Sigma, #MAK038-1KT). Standard protocols were followed according to the manufacturers' instructions. Values were normalized to the total protein concentration, measured by BCA assay (ThermoFisher Scientific, #23225).

Analysis of GSH and GSSG by liquid chromatography-mass spectrometry (LC-MS)

To determine the relative abundance of glutathione (GSH) and glutathione disulfide (GSSG) in mouse heart tissues, cardiac extracts were prepared and analyzed by ultra-high resolution mass spectrometry (HRMS). Briefly, approximately 10 mg of individual tissue samples were homogenized with Precellys Tissue Homogenizer. Metabolites were extracted using ice-cold 0.1% trichloroacetic acid in 90/10 (v/v) Acetonitrile/water. Then, extracts were centrifuged at 17,000 *g* for 5 minutes at 4°C, and supernatants were transferred to clean auto sampler vials. In the end, 10 μL volume of each sample was injected for analysis by liquid chromatography-mass spectrometry (LC-MS). Thermo Vanquish LC system included a SeQuant Zic-cHilic column (3 μm particle size,

100 × 2.1 mm) with column compartment kept at 30°C. Mobile phase A (MPA; weak) was 95/5 (v/v) acetonitrile/(200 mM ammonium acetate buffer, pH 5.8), and mobile phase B (MPB; strong) was 50/45/5 acetonitrile/water/(200 mM ammonium acetate buffer, pH 5.8). Autosampler tray was chilled to 4°C. The mobile phase flow rate was 300 µL/min, and the gradient elution program was: 0-2 minutes, 20% MPB; 2-6 minutes, 20-80% MPB; 6-10 minutes, 80% MPB; 10-11 minutes, 80-20% MPB. The total run time was 15 minutes. Data were acquired using a Thermo Orbitrap Fusion Tribrid Mass Spectrometer under the ESI positive ionization mode at a resolution of 240,000. Raw data files were imported to Thermo Trace Finder software for final analysis. The relative abundance of each metabolite was normalized by tissue weight.

Immunoblotting

Total proteins were extracted from cultured cardiomyocytes or cardiac tissues using RIPA lysis and extraction buffer (ThermoFisher Scientific, #89900), supplemented with protease and phosphatase inhibitors (ThermoFisher Scientific, #88669). Protein concentration was determined with a BCA kit (ThermoFisher Scientific, #23225). Equal amount of total proteins for individual samples was loaded on Criterion TGX precast gels (Bio-Rad, 4-20%, #5671095) and transferred onto nitrocellulose membranes (Bio-Rad, #1704157). After blocking for 1 hour at room temperature in 5% non-fat milk or 3% BSA, membranes were incubated with primary antibodies overnight at 4°C, followed by incubation with fluorescent dye-labeled secondary antibodies at room temperature for 1 hour. After washing with TBS-Tween 20, blots were scanned with an Odyssey scanner (Li-Cor). The following antibodies were used: GAPDH, Fitzgerald, #10R-G109A; Rcan1, Sigma, #D6694; ATF4, CST, #11815; ANF, Abcam, #ab180649; caspase 3, CST, #9662; cleaved caspase 3, CST, #9664; IRDye 800 CW goat anti-rabbit secondary antibody, Li-Cor, #925-32211; Alexa Fluor 700-conjugated goat anti-mouse secondary antibody, ThermoFisher Scientific, #A-21036.

Chromatin immunoprecipitation (ChIP) assay

ChIP assay was performed using an EZ-ChIP kit (Millipore, #17-371). Briefly, H9c2 cells were first infected with adenoviruses expressing ATF4. Cells were cross-linked with 1% formaldehyde, lysed with SDS lysis buffer, and subjected to sonication to shear genomic DNA. Cross-linked protein/DNA complexes were precipitated using ATF4 antibody (CST, #11815) with normal rabbit IgG antibody (CST, #3900S) as control. PCR was then conducted to detect specifically bound DNA fragments.

Histology and immunostaining

Mouse hearts were harvested and fixed in 10% neutralized formalin for 48 hours at 4°C. Paraffin sections (5-µm thickness) were prepared. Hematoxylin and eosin (H&E) staining and Masson's Trichrome staining were conducted by the Molecular Pathology Core at UTSW. TUNEL staining was performed according to the manufacturer's recommendations (Promega, DeadEnd fluorometric TUNEL system, #G3250).

For immunofluorescence staining, tissue sections were first deparaffinized and rehydrated. Antigens were retrieved with antigen retrieval solution (BioGenex, #HK086-9K), and non-specific binding was blocked by incubating with normal goat serum.

Primary antibodies were used to incubate overnight at 4°C. Sections were then stained with secondary antibodies for 1 hour at room temperature. After six washes with PBS, sections were counterstained by ProLong Gold antifade reagent with 4,6-diamidino-2-phenylindole (ThermoFisher Scientific, #P36935), and images were captured by a fluorescent microscope. The following antibodies were used: Troponin T, cardiac isoform Ab-1 (Clone 13-11) mouse monoclonal antibody, ThermoFisher Scientific, #MS-295-P1; 4-hydroxy-nonenal, Abcam, #ab46545, goat anti-rabbit secondary antibodies Alexa Fluor 488, ThermoFisher Scientific, #A-11008; goat anti-mouse secondary antibodies Alexa Fluor 568, ThermoFisher Scientific, #A-11011. Secondary antibody-only staining was used as negative controls. Histological images with the least processing artifact and denoting relatively similar cell number for each antibody or similar anatomy were chosen as representative images for main and online figures.

RNA isolation, reverse transcription, and quantitative PCR

Total RNAs from cardiac tissues and NRVMs were isolated with an Aurum Total RNA Fatty and Fibrous Tissue kit (Bio-Rad, #732-6870) and a Quick-RNA Microprep kit (Zymo Research, #R1051), respectively. A total of 200-250 ng RNAs of each sample were used for reverse transcription (Bio-Rad, iScript, #1708891), and cDNAs were then diluted by 10-fold with ddH_2O. For each sample, 2 µL diluted cDNAs was used for quantitative PCR to determine relative mRNA level to 18s rRNA using a LightCycler machine (Roche) and SYBR green reagent (Bimake, #B21203). All primers are listed in Supplemental Table S1. RNA-sequencing was conducted by Psomagen Inc. and Novogen as before.[49] All raw bulk RNA-sequencing data are deposited in the Gene Expression Omnibus (GEO): GSE187005.

Analysis of polar metabolites by ion chromatography-mass spectrometry (IC-MS)

To assess the relative abundance of polar metabolites in primary cardiomyocytes, we seed approximately 2×10^6 NRVMs in each 100 mm dish. We overexpressed ATF4 by adenovirus infection with LacZ as control. Metabolites were extracted with 1 mL ice-cold 0.1% ammonium hydroxide and 2 mM $^{13}C_3$-lactate (as internal standard) in 80/20 (v/v) methanol/water. Extracts were centrifuged at 17,000 *g* for 5 minutes at 4°C, and supernatants were transferred to clean tubes and evaporated with a SpeedVac concentrator. Pellets were used for DNA measurements and normalization.

Dried extracts were reconstituted in deionized water, and 10 µL of each sample was used for analysis by ion chromatography-mass spectrometry (IC-MS). The IC mobile phase A (MPA, weak) was water, and the mobile phase B (MPB, strong) was water containing 100 mM KOH. A Thermo Scientific Dionex ICS-5000+ system including a Thermo IonPac AS11 column (250 × 2 mm, 4 µm particle size) with the column compartment kept at 30°C was used. The autosampler tray was chilled to 4°C. The mobile phase flow rate was 360 µL/min, and the gradient elution program was: 0-5 minutes, 1% MPB; 5-25 minutes, 1-35% MPB; 25-39 minutes, 35-99% MPB; 39-49 minutes, 99% MPB; 49-50 minutes, 99-1% MPB. The total run time for each sample was 50 minutes. To assist desolvation for better sensitivity, methanol was delivered by an external pump and combined with the eluent via a low dead volume mixing tee. Raw data were acquired with a Thermo Orbitrap Fusion Tribrid Mass Spectrometer under

ESI negative ionization mode at a resolution of 240,000. Raw data files were imported to Thermo Trace Finder software for analysis. The relative abundance of each metabolite was normalized by $^{13}C_3$-lactate and DNA level.

Metabolites profiles were first analyzed using MetaboAnalyst 5.0,[21] utilizing univariate built-in analytical methods from modules of this web-based platform. Multi-omics analysis was performed utilizing the Joint Pathway Analysis (JPA) module from MetaboAnalyst 5.0 that enables the combination of transcriptomics and metabolomics data for functional enrichment analysis and pathway topology analysis.[21] We entered the differentially expressed genes and metabolites, with optional log fold changes. For parameter setting, we choose “Hypergeometric Test” for enrichment analysis, “Degree Centrality” for topology measure, and “Combine Queries” for integration method.

Metabolic tracing in NRVMs

To determine the incorporation of glucose carbons into glycolysis, the pentose phosphate pathway, serine biosynthesis, and the tricarboxylic acid cycle, extracts were prepared and analyzed by high-resolution mass spectrometry. Briefly, approximately 2 × 10^6 NRVMs were seeded in each 100 mm dish. ATF4 was overexpressed by adenovirus infection along with control GFP adenoviruses. After 24 hours, we aspirated medium and add 8 mL of stable isotope tracer solution containing 11.1 mM 1,2-$^{13}C_2$-glucose the measure the pentose phosphate pathway or U-^{13}C-glucose to measure serine biosynthesis. After another 24 hours, metabolites were extracted using 1 mL ice-cold 0.1% ammonium hydroxide in 80/20 (v/v) methanol/water and processed for IC-MS. The relative abundance of each metabolite was normalized by total peak intensity. The fractional abundance of each isotopologue was calculated by the peak area of the corresponding isotopologue normalized by the sum of all isotopologue areas.[50]

Cell death assay

After hypertrophy treatment and siRNA silencing, cells were collected (including floating dead cells) and stained with 1 μg/mL propidium iodide (ThermoFisher Scientific, #P1304MP). The percentage of propidium iodide-positive dead cells was analyzed using a FACScan flow cytometer and quantified with Flowjo 10.7.2.

Statistical analysis

All data are represented as mean±SEM. No statistical analysis was performed to pre-determine sample sizes. Sample size and only within-test corrections were made based on our previous experience, experimental approach, availability, and feasibility required to obtain statistically significant results. Normality of distribution was assessed by using Shapiro-Wilk test. Normally distributed data were then analyzed with unpaired, 2-tailed Student’s t test to compare differences between two groups. For multiple group comparisons with 1 variable, one-way ANOVA was performed, followed by Dunnett or Tukey’s multiple comparisons test. For multiple group comparisons with more than 2 variables, two-way ANOVA was conducted, followed by Tukey’s multiple comparisons test. For data not following a normal distribution, unpaired 2-tailed Mann-Whitney test (2 groups) or Kruskal-Wallis test (3 or more groups) was used, followed by Dunn post hoc test. A P value of <0.05 was considered statistically significant. Statistical analyses were conducted with Graphpad Prism 8.4.3.

Supplemental Table S1. Primers used in this study.

Gene	Species	Primer (forward/reverse)	Test
$ATF4^{F/F}$	mouse	GCAGACGTTCCTGGGTTAGA/GCTTCCTGCCTACATTGCTC	genotyping
Cre		GATTTCGACCAGGTTCGTTC/GCTAACCAGCGTTTTCGTTC	genotyping
18s	rat	AAACGGCTACCACATCCAAG/CCTCCAATGGATCCTCGTTA	qPCR
MTHFD2	rat	GCAGGTCCAAAAACGTTGGG/CGTCGATGACTGTTGCTCCT	qPCR
G6PDX	rat	ACAAGCACCTCAACAGCCAC/TGATTGGAGCTCTGCAGGTC	qPCR
PHGDH	rat	GGAGGAGCTGATAGCCGAAC/TTGGGGGTGTTCATGACGAG	qPCR
PSAT1	rat	AGCTGCCGTACTCGGTATTG/TTAAGGGGACGGCACTGAAC	qPCR
MTHFD2L	rat	TGGCTTGTCGCTGCTCC/AAGCCACGATTCCACACCTT	qPCR
MTHFD1L	rat	GGTGCCCAATGTTGTTGTCC/ACCAGGTCAATCTCTGCACG	qPCR
ALDH1L2	rat	CATCAACCCCACAGACGGAA/ATCCAGCGCTTCTATGGTCG	qPCR
MTHFD1	rat	CGGGAATCCTGAACGGGAAA/GTGAGTGGCTTTGATCCCGA	qPCR
MTHFR	rat	AACGAGGCCAGAAGAAGTGG/GTGACATCCACGAAGAGGGG	qPCR
DHFR	rat	GCATTGGCAAGAACGGAGAC/GCTCCTTGTGGTGGTTCCTT	qPCR
ME1	rat	CCCGCATCTCAACAAGGACT/TCAGAGTTCAGACGCTCGAAA	qPCR
ME2	rat	TGTATCAGAAGCGAGACCGC/TGCAGCAGTCCCTTGAATGT	qPCR
ME3	rat	GAAGTGCTACCAGGTCACCG/TGATATTCCAGGCAGCCACC	qPCR
IDH1	rat	CAACGGTACCATCCGGAACA/TGCGACCCATCTTTTGGTGT	qPCR
IDH2	rat	TCGAGCTGGCATGTTCAAGT/TTGGTGCTCAAGTAGAGCGG	qPCR
GDH1	rat	ATCCAATGCACCCAGAGTCA/ACGGACATGAGCAAGTGGTA	qPCR
NNT	rat	TAGCAGCTCTCTACGGTGGT/CCTCCTGCAACCCCAATCAT	qPCR
SHMT1	rat	CACTGATTGGGCCGCTCTA/GCTGTAAACCTCAGCATCGC	qPCR
SHMT2	rat	TGTGGTCAGCTGGTCTGC/GTTGTTGAGACAGGACCCCA	qPCR
ATF4	rat	ACCAGACAGTCTGCCTTCTC/CTCTTCTTCTGGCGGTACCT	qPCR
18s	mouse	AGGGTTCGATTCCGGAGAGG/CAACTTTAATATACGCTATTGG	qPCR
ANF	mouse	CTTCTTCCTCGTCTTGGCCT/CTGCTTCCTCAGTCTGCTCA	qPCR
BNP	mouse	CATGGATCTCCTGAAGGTGC/CCTTCAAGAGCTGTCTCTGG	qPCR
COL1A	mouse	CTCGTGGATTGCCTGGAACA/CCAACAGCACCATCGTTACC	qPCR
TGFβ	mouse	ATGGCTCTCCTTCGACGTGA/AATCTCGCCTCGAGCTC	qPCR
CTGF	mouse	TGCACTTGCCTGGATGG/GGCAGTTGGCTCGCATCATA	qPCR
G6PD	mouse	GGCCAGTATGATGATGCAGC/CTTCTCCACGATGATGCGGT	qPCR
PHGDH	mouse	GACGTGAACTTGGTGAACGC/CTGGTCTGAAGACAGCTCCG	qPCR
PSAT1	mouse	GGAGCGCCAGAATAGAAGCA/TCTTCGGTTGTGACAGCGTT	qPCR
MTHFD2	mouse	TGTCATTAACGTGGGGCGAA/TCAGCTGCTCTTTGGGAGTG	qPCR
MTHFD1L	mouse	TCAAGGCTGGACCCCTTCTA/CCCATGTGCTTTTCGCTACG	qPCR
ALDH1L1	mouse	CACCTTCGGGGACTTCATCC/TGACACTTCCATCCGTTGGG	qPCR
ALDH1L2	mouse	CCCAGTACTTTTCTGCGGGT/ACTTGGTGGCCATGTAGACG	qPCR
MTHFD1	mouse	TCTGCGCAAATCAGGGATCG/TCATCTCTGTCGCCAACCTG	qPCR
MTHFR	mouse	ACCTCTCTGGAGAGCCGAAT/TTTGCGTTGATGTTGGGCTG	qPCR
TYMS	mouse	TTCAAGAAGGAGGACCGCAC/TGTCGGGCAGAAAATCCCAA	qPCR
DHFR	mouse	CCCAGCATATGCACAGGGTA/TGCCCTTTGGACTTACCTGC	qPCR
ME1	mouse	CGCATCTCAACAAGGACTTGGC/CGCATCTCAACAAGGACTTGGC	qPCR
ME2	mouse	GCCAGAAAATCATGTTAAGGCTGT/ACTTCTCGGGCTGTATCCCT	qPCR
ME3	mouse	GACCCGTACCCCTGAAGAAG/GTTGCGGTCTTGGAGAGTCA	qPCR
IDH1	mouse	AGGAGGTTCTGTGGTGGAGA/ACTTGACGCCCACGTTGTAT	qPCR
IDH2	mouse	GGACAGTCACCCGCCATTAC/ACATTGCTGAGGCCATGGAT	qPCR
GDH1	mouse	GCCAGCATCGTAGAGGACAA/CACGTCAGTGCTGTAACGGA	qPCR
GDH2	mouse	ATGCTGGAGGAGTAACAGTG/ATTGTGTAGGCCAAGCCAGA	qPCR
NNT	mouse	TGAAACGACTAAGCCGGGAG/CTTCATCACCACGGTCCCTC	qPCR
SHMT1	mouse	GAGAATTTTGCCAGCCGAGC/GCCTGTAATGCACGCTTCTG	qPCR
SHMT2	mouse	ACTCACAAGACACTGCGAGG/GTACTCGCGGAACATAGGGG	qPCR
ATF4	mouse	CCACCAGACAATCTGCCTTC/CTAGCTCCTTACACTCGCCA	qPCR
MTHFD2	rat	ACAGCCAGAGCAAACGACAG/CCTCCTCTCCAGTCCCATACT	ChIP
MTHFD2	rat	AACTTGCTGGCCTTGTTTCAC/GAACTTCAGCTCAAGGGGGAT	ChIP remote
G6PDX	rat	CCCTCACACTGCAACCTTTAC/GCACCTCTGGAAGAATCAGTTG	ChIP
G6PDX	rat	ACCCTGGCTTCCAGAGTAGA/GCCTGCCTCCTGCATTTAGT	ChIP remote

Supplemental Figure S1

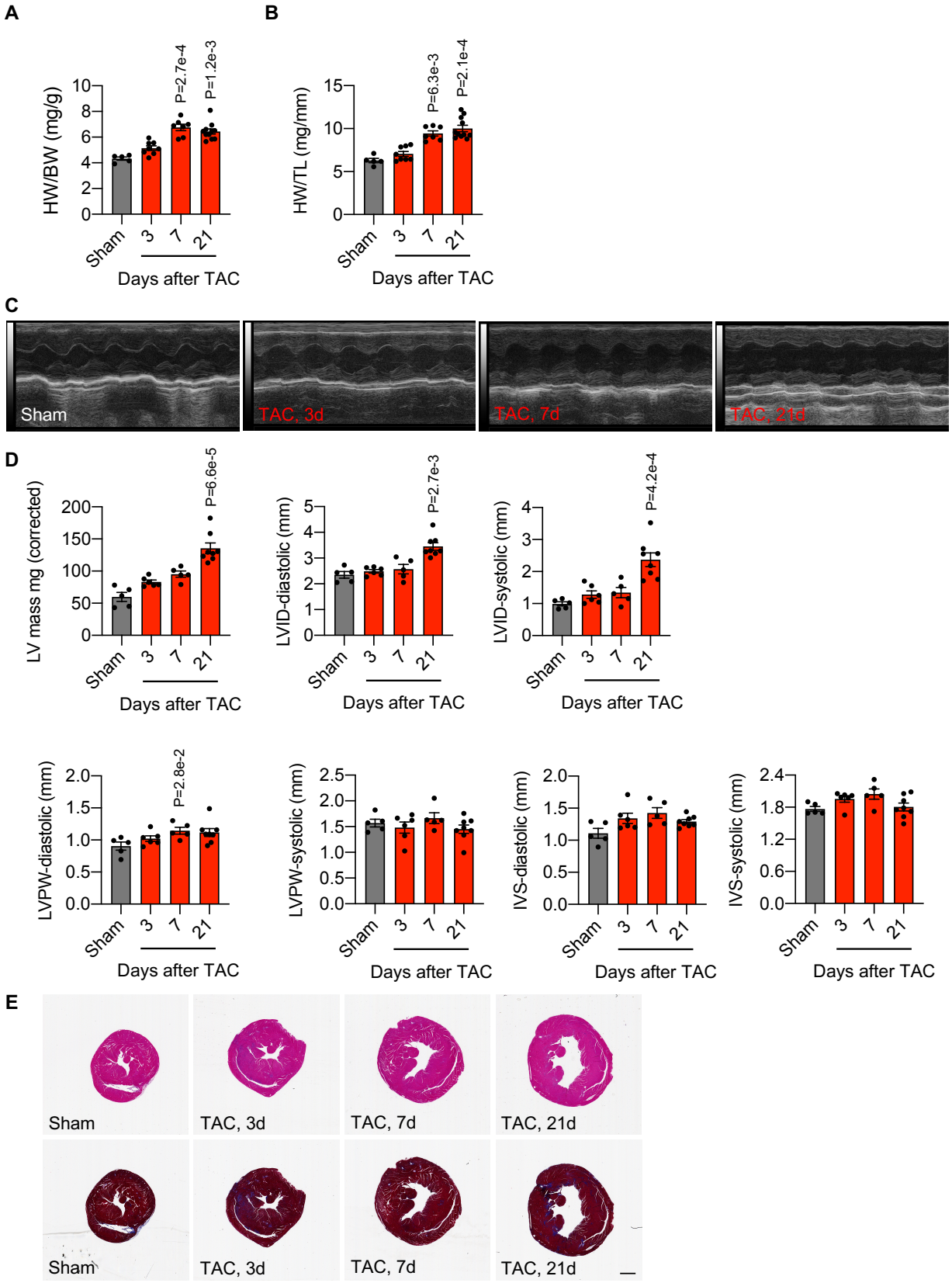

Supplemental Figure S1. Pressure overload induces cardiomyopathy and heart failure in mice.

- **A.** Wild-type mice of 8 weeks old were used for sham or transverse aortic constriction (TAC). The heart was harvested at different times after surgery. TAC led to significant increases in the ratio of heart weight/body weight (HW/BW) as indication of cardiac hypertrophic growth. Sham, n=5; 3 days after TAC, n=8; 7 days after TAC, n=7; 21 days after TAC, n=11.
- **B.** The ratio of heart weight/tibia length (HW/TL) was elevated by TAC. Sham, n=5; 3 days after TAC, n=8; 7 days after TAC, n=7; 21 days after TAC, n=11.
- **C.** Representative echocardiography images (M mode) are shown.
- **D.** LV (left ventricular) mass was increased by pressure overload. LVID (Left ventricular inner diameter) was augmented by TAC at both systole and diastole, whereas LVPW (left ventricular posterior wall) and IVS (interventricular septum) were largely maintained. Sham, n=5; 3 days after TAC, n=6; 7 days after TAC, n=5; 21 days after TAC, n=8.
- **E.** TAC caused cardiac hypertrophy at the histological level. Hematoxylin & eosin (H&E) staining and Masson's Trichrome staining were conducted. Scale: 1 mm.

Kruskal-Wallis test was conducted, followed by Dunn's test to determine statistical significance for comparisons of the means of each surgical group (3, 7, and 21 days after TAC) with the mean of the sham group (**A, B, D**). Data are represented as mean±SEM.

Supplemental Figure S2

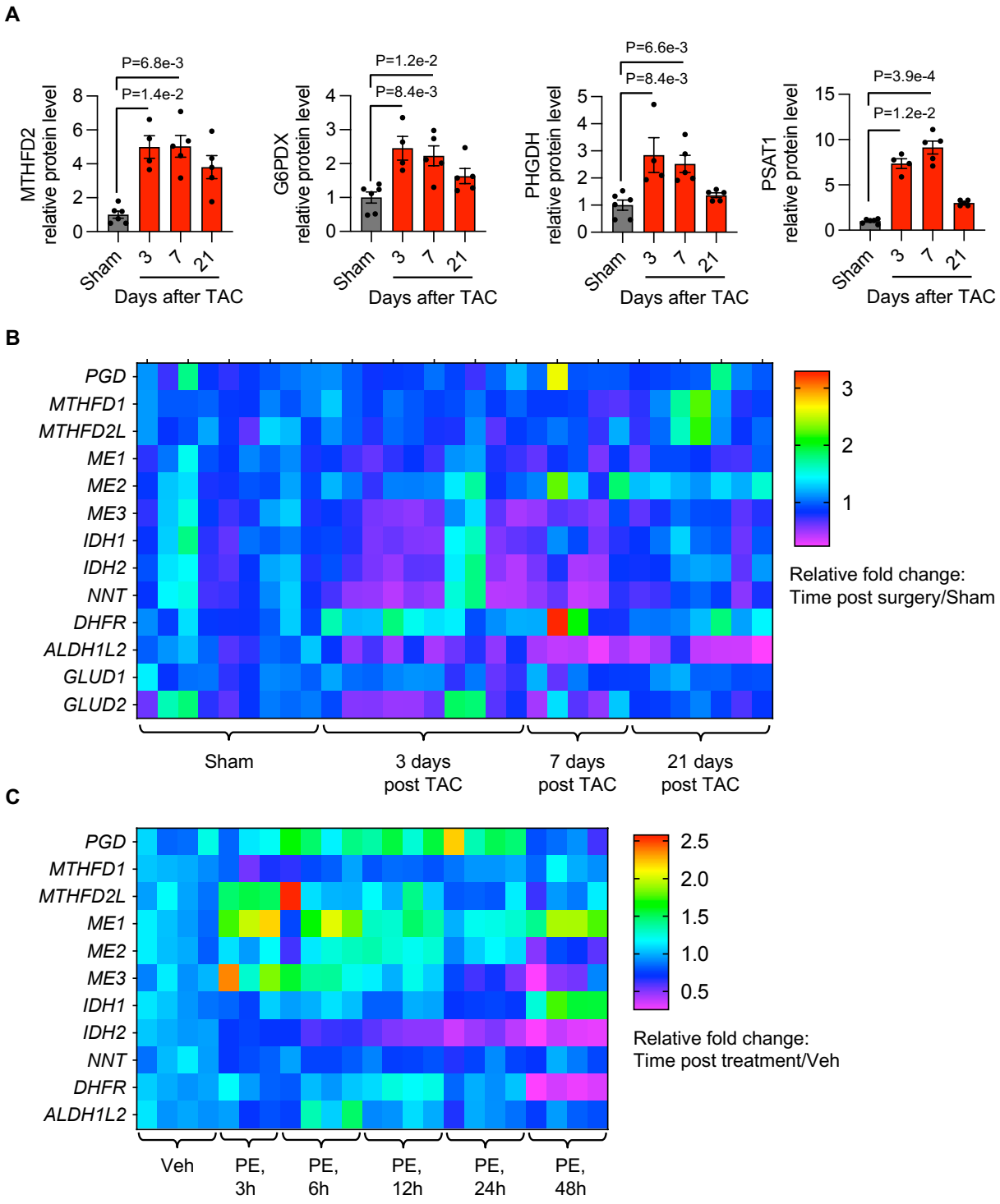

Supplemental Figure S2. Cardiomyocyte hypertrophic growth induces NADPH synthesis signaling and the pentose phosphate pathway.

- **A.** Quantification of the protein level of MTHFD2, G6PDX, PHGDH, and PSAT1 showed a significant increase under pressure overload. Sham, n=6; 3 days after TAC, n=4; 7 days after TAC, n=5; 21 days after TAC, n=5.
- **B.** Multiple genes involved in NADPH production and the pentose phosphate pathway (PPP) were analyzed in the heart after TAC. Sham, n=9; 3 days after TAC, n=10; 7 days after TAC, n=5; 21 days after TAC, n=8.
- **C.** Multiple genes of NADPH generation pathways and the PPP were determined at the mRNA level in neonatal rat ventricular myocytes (NRVMs) after phenylephrine (PE) treatment. Vehicle (Veh), n=4; PE, 3h, n=3; PE, 6h, n=4; PE, 12h, n=4; PE, 24h, n=4; PE, 48h, n=4.

Kruskal-Wallis test was conducted, followed by Dunn's test to determine statistical significance for comparisons of the means of each surgical group (3, 7, and 21 days after TAC) with the mean of the sham group (**A**). Gene expression at the protein level from each surgical group (3, 7, and 21 days after TAC) was normalized to the mean of the sham group, which was set to 1 (**A**). Data are represented as mean±SEM.

Supplemental Figure S3

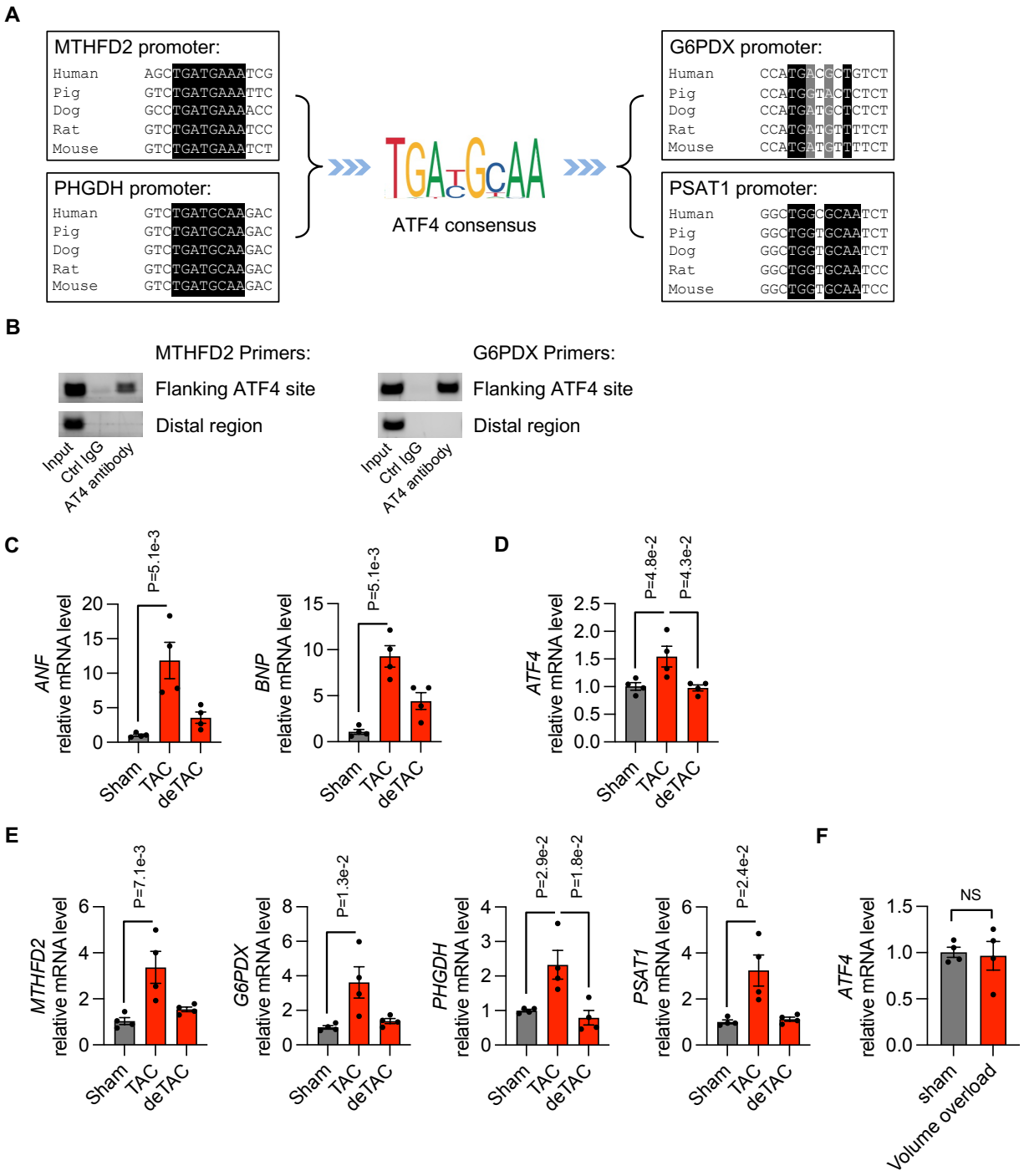

Supplemental Figure S3. ATF4 controls multiple genes involved in NADPH biosynthesis.

- **A.** Promoter analysis identified ATF4 as a common upstream transcription factor of *MTHFD2* and *PHGDH*. ATF4 consensus binding sites were further identified in the promoters of *G6PDX* and *PSAT1*, respectively.
- **B.** Chromatin immunoprecipitation (ChIP) assay showed that ATF4 bound the promoters of *MTHFD2* and *G6PDX*. Primers designed at the distal region of respective promoters were used as negative controls.
- **C.** After TAC, deTAC was conducted. Hypertrophic marker gene expression was induced by TAC, and this elevation was diminished by deTAC. N=4 for each group.
- **D.** The increased expression of *ATF4* after TAC was reduced by deTAC. N=4 for each group.
- **E.** Pressure overload by TAC caused an increase in the expression of *MTHFD2*, *G6PDX*, *PHGDH*, and *PSAT1*. This increase was reversed by deTAC. N=4 for each group.
- **F.** Volume overload did not affect the mRNA expression of *ATF4* in the heart. NS, not significant. N=4 for each group.

Kruskal-Wallis test was conducted, followed by Dunn's test to determine statistical significance for comparisons of the means of each surgical group (TAC, deTAC, and volume overload) with the mean of the sham group (**C-E**). Gene expression at the mRNA level from each surgical group (TAC, deTAC, and volume overload) was normalized to the mean of the sham group, which was set to 1 (**C-E**). Data are represented as mean±SEM.

Supplemental Figure S4

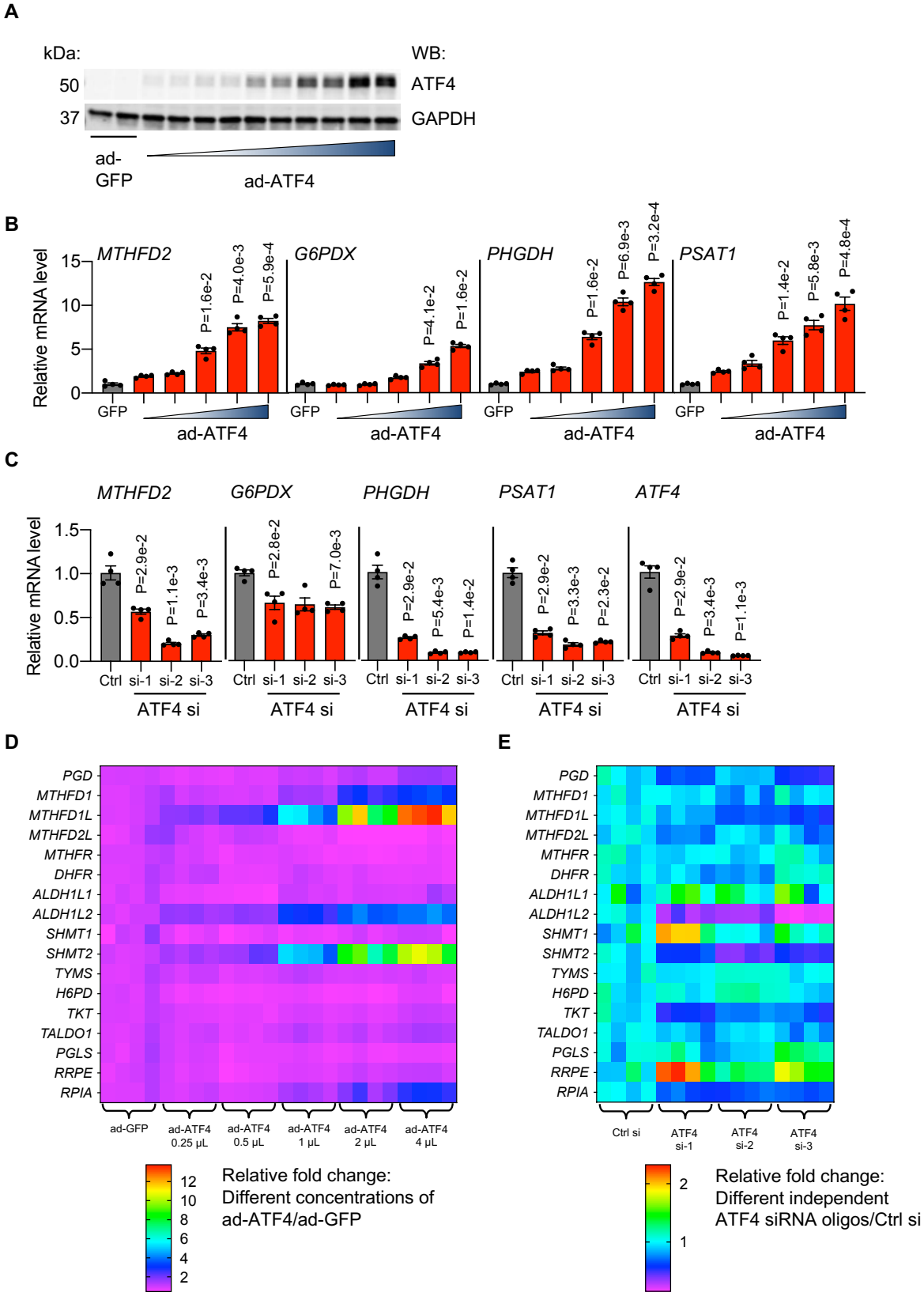

Supplemental Figure S4. ATF4 governs genes of NADPH production pathways and the PPP.

- **A.** ATF4-expressing adenoviruses were used to infect NRVMs. ATF4 protein expression was increased in a dose-dependent manner.
- **B.** ATF4 overexpression stimulated the mRNA level of *MTHFD2*, *G6PDX*, *PHGDH*, and *PSAT1*, respectively. N=4 for each group.
- **C.** ATF4 silencing in NRVMs decreased the mRNA level *MTHFD2*, *G6PDX*, *PHGDH*, and *PSAT1*, respectively. Three independent siRNA oligos against *ATF4* were used. N=4 for each group.
- **D.** NRVMs was infected by adenoviruses expressing ATF4 or control GFP. Different MOIs were used. Heatmap showed other genes of the NADPH generation pathways and the PPP. N=4 for each group.
- **E.** ATF4 was silenced by 3 independent siRNA oligos. Gene expression was determined by quantitative RT-PCR. N=4 for each group. Note that *MTHFD1L*, *SHMT2*, and *ALDH1L2* also showed consistent upregulation and downregulation in ATF4 overexpression and knockdown NRVMs, respectively.

Kruskal-Wallis test was conducted, followed by Dunn's test to determine statistical significance for comparisons of the means of each ad-ATF4 treatment group (different concentrations of ad-ATF4) with the mean of the ad-GFP control group (**B**) and to determine statistical significance for comparisons of the means of each ATF4 siRNA treatment group (independent ATF4 siRNA oligos used) with the mean of the Ctrl si group (**C**). Gene expression at the mRNA level from each ad-ATF4 treatment group (different concentrations of ad-ATF4) group was normalized to the mean of the ad-GFP control group, which was set to 1 (**B**). Gene expression at the mRNA level from each ATF4 siRNA treatment group (independent ATF4 siRNA oligos used) was normalized to the mean of the control (Ctrl) si group, which was set to 1 (**C**). Data are represented as mean±SEM.

Supplemental Figure S5

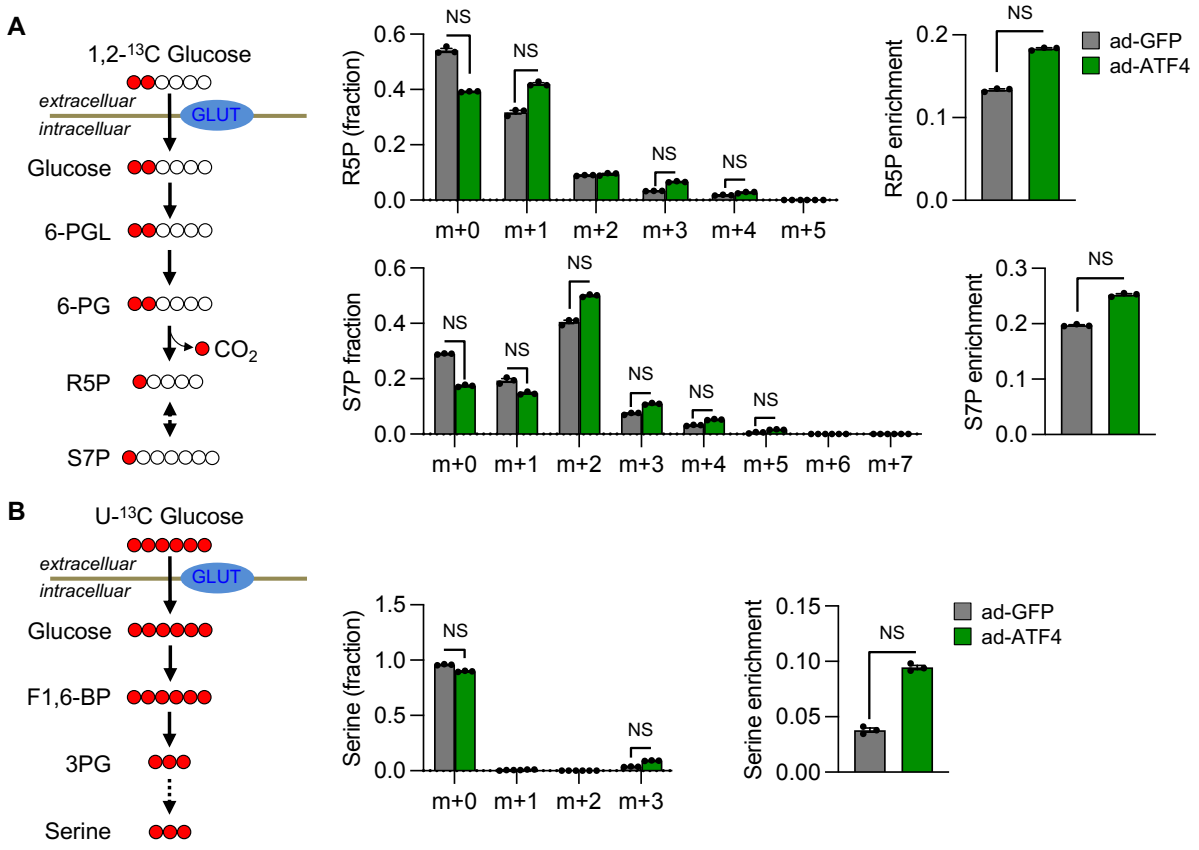

Supplemental Figure S5. ATF4 enhances the metabolic flux of the pentose phosphate pathway (PPP) and serine biosynthesis.

- **A.** NRVMs were infected by adenoviruses that expressed ATF4 or GFP control. Stable isotope labeled glucose (1,2-^{13}C glucose) was included in culture media for 24 hours. Metabolomics analysis was conducted to determine the flux of the PPP. NS, not significant. N=3 for each group.
- **B.** U-^{13}C glucose was used to measure the flux of serine biosynthetic pathway in NRVMs after ATF4 overexpression. NS, not significant. N=3 for each group.

6-PGL, 6-phosphogluconolactone; 6-PG, 6-phosphogluconate; R5P, ribose 5-phosphate; S7P, Sedoheptulose 7-phosphate; F1,6-BP, fructose 1,6-biphosphate; 3PG, 3-phosphoglycerate.

Mann-Whitney test was conducted between the ad-GFP control group and ad-ATF4 group (**A-B**). Data are represented as mean±SEM.

Supplemental Figure S6

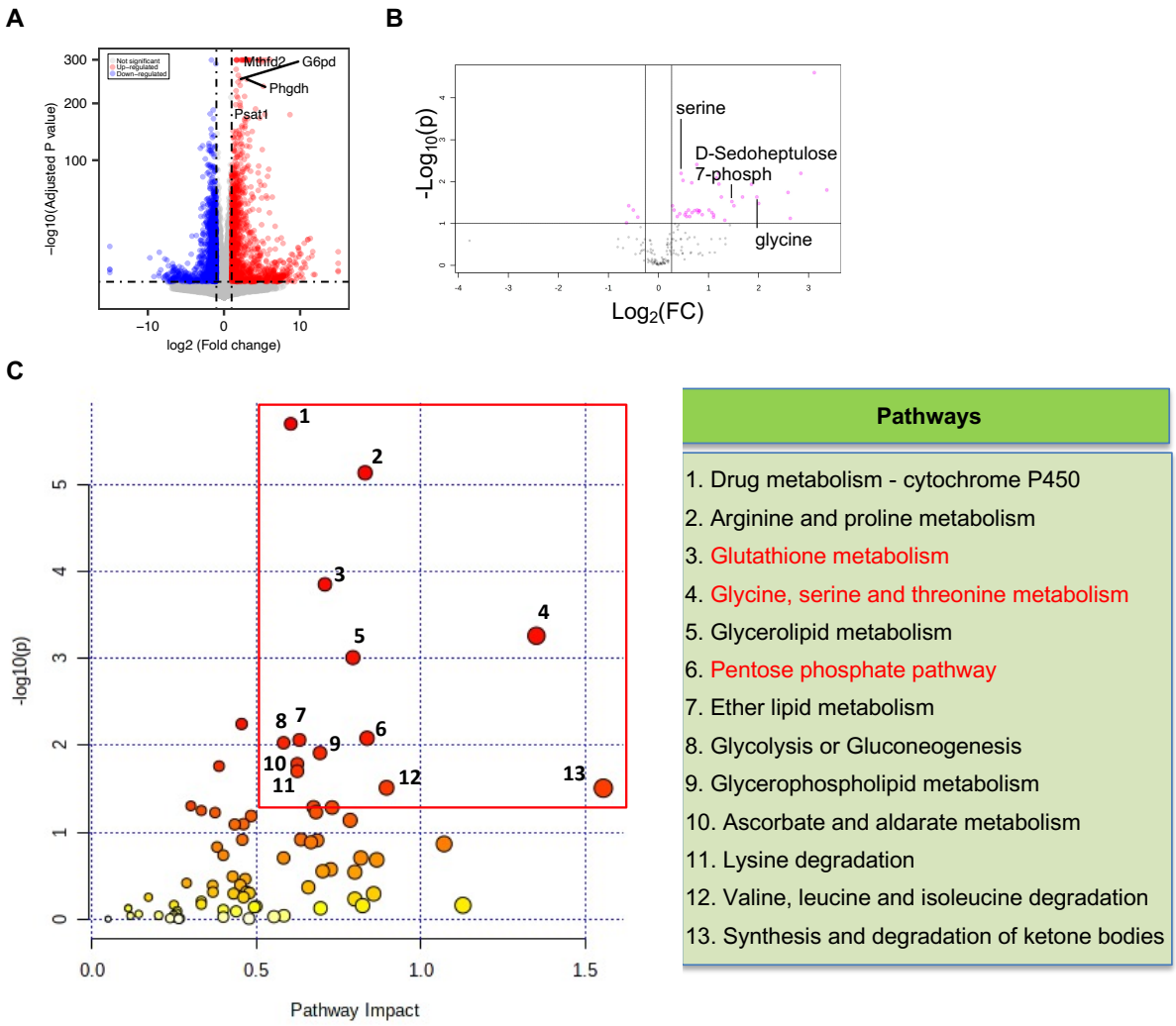

Supplemental Figure S6. ATF4 stimulates the PPP and pathways involved in redox control.

A. The volcano plot of RNA-sequencing results. The 4 targets of ATF4 are labeled.
B. Three metabolites relevant to redox control are selected to show their changes between GFP and ATF4 adenovirus infection in NRVMs. FC, fold change.
C. The result of joint pathway analysis (JPA) using transcriptomic and metabolomic data is shown. Red box highlights the top pathways that were significantly impacted by ATF4 overexpression as defined by enrichment significance $P<0.05$ [$-\log(P)>1.3$] and pathway impact >0.5.

Supplemental Figure S7

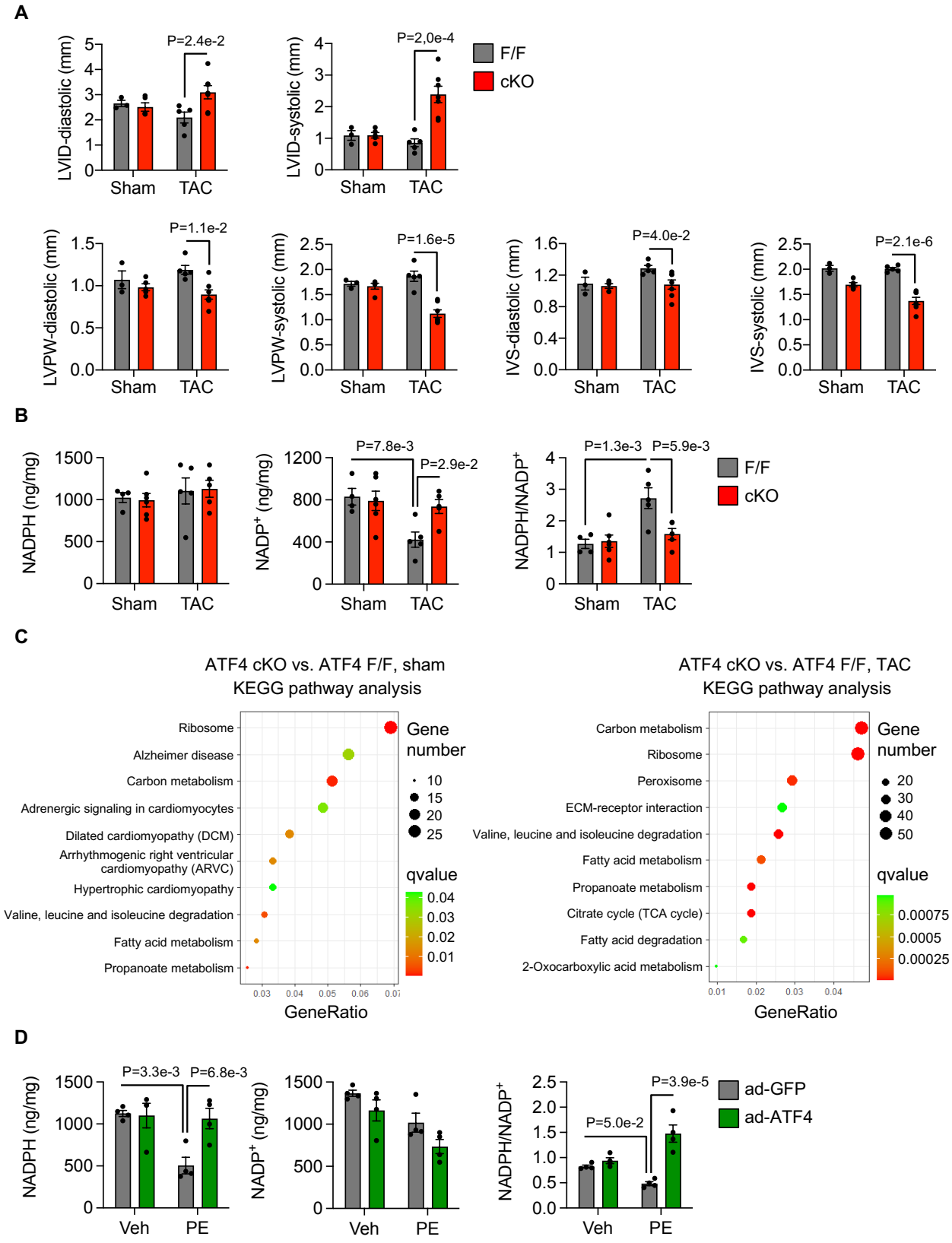

Supplementary Figure S7. Cardiomyocyte specific ATF4 deletion exacerbates cardiac dysfunction under pressure overload.

- **A.** Echocardiography analysis was performed to examine cardiac function 7 days after sham or TAC. Sham, F/F, n=3; Sham, cKO, n=5; TAC, F/F, n=5; TAC, cKO, n=7.
- **B.** ATF4 cKO hearts showed a decrease in the ratio of NADPH to $NADP^+$ 1 day after TAC. Sham, F/F, n=4; Sham, cKO, n=6; TAC, F/F, n=6; TAC, cKO, n=5.
- **C.** Control ($ATF4^{F/F}$) and ATF4 cKO mice were subjected to either sham or TAC. A week later, cardiac tissues were harvested and total RNAs were extracted for RNA-sequencing. The top 10 most enriched pathways by KEGG analysis are shown. N=3 for each group.
- **D.** ATF4 overexpression in NRVMs was achieved by adenovirus infection (ad-ATF4) using ad-GFP as a negative control. Phenylephrine (PE, 50 μM) treatment was conducted for 12 hours, and cells were harvested. ATF4 overexpression increased cellular NADPH level and the ration of NADPH to $NADP^+$ after PE treatment. N=4 for each group.

Two-way ANOVA was conducted, followed by Tukey's multiple comparisons test (**A-B, D**). Data are represented as mean±SEM.